

Green Chemistry

Accepted Manuscript



This is an *Accepted Manuscript*, which has been through the Royal Society of Chemistry peer review process and has been accepted for publication.

Accepted Manuscripts are published online shortly after acceptance, before technical editing, formatting and proof reading. Using this free service, authors can make their results available to the community, in citable form, before we publish the edited article. We will replace this *Accepted Manuscript* with the edited and formatted *Advance Article* as soon as it is available.

You can find more information about *Accepted Manuscripts* in the [Information for Authors](#).

Please note that technical editing may introduce minor changes to the text and/or graphics, which may alter content. The journal's standard [Terms & Conditions](#) and the [Ethical guidelines](#) still apply. In no event shall the Royal Society of Chemistry be held responsible for any errors or omissions in this *Accepted Manuscript* or any consequences arising from the use of any information it contains.



www.rsc.org/greenchem

**Characterization of Organosolv Switchgrass Lignin by Using High Performance Liquid
Chromatography / High Resolution Tandem Mass Spectrometry Using Hydroxide-Doped
Negative-Ion Mode Electrospray Ionization**

Tiffany M. Jarrell[†], Christopher L. Marcum[†], Huaming Sheng[†], Benjamin C. Owen[†], C.
J. O'Lenick[‡], Hagen Maraun[‡], Joseph J. Bozell[‡], and Hilikka I. Kenttämäa^{†*}

[†] *Department of Chemistry, Purdue University, West Lafayette, IN*

[‡] *University of Tennessee, Center for Renewable Carbon, Knoxville, TN*

*Corresponding Author
Professor Hilikka I. Kenttämäa
Department of Chemistry
Purdue University
West Lafayette, IN, 47907
Tel: (765) 494-0882
Fax: (765) 494-9421
Email: hilkka@purdue.edu

ABSTRACT

Lignin is an aromatic biopolymer that may yield valuable chemicals currently obtained solely from petroleum. However, extraction of lignin by using traditional methods, such as organosolv extraction, produces very complex mixtures. Molecular level characterization of the major components is essential to be able to rationally tailor methodology for the conversion of these mixtures to transportation fuel and valuable chemicals. In this study, high performance liquid chromatography/high resolution tandem mass spectrometry (HPLC/MSⁿ) was used to obtain molecular weight, elemental composition and structural information for the major components in an organosolv lignin sample. HPLC/MSⁿ coupled with hydroxide-doped electrospray ionization was used to identify the structures of the major components by using a Thermo Scientific linear quadrupole ion trap - Fourier transform ion cyclotron resonance hybrid mass spectrometer (LQIT/FT-ICR). The results reported here demonstrate that the major products of organosolv extraction are low molecular weight compounds, monomeric and dimeric lignin units, with various functionalities.

INTRODUCTION

The conversion of biomass to valuable aromatic and aliphatic compounds may provide a viable replacement for petroleum as a source of these compounds.¹⁻⁹ Biomass is usually processed by first separating it into its primary components, hemicellulose, cellulose, and lignin.^{7, 8, 10, 11} Lignin is a biopolymer found in the cell wall of plants and it is composed of phenolic units with diverse structural motifs.¹² Lignin is currently being explored as a source of valuable aromatic chemicals.^{12, 13} Therefore, the extraction, degradation, and transformation of lignin are being explored with vigor.^{13, 14} Organosolv is a pulping approach that utilizes organic solvents to solubilize lignin and hemicelluloses. The solution is separated into an aqueous and organic phase upon addition of a brine solution. The organic phase contains the lignin fraction.^{5, 7, 15} This method was developed as an alternative to the Kraft method, which requires the use of sodium hydroxide or sodium sulfide, to enable the use of solvents that can be recovered through distillation and to eliminate harmful wastes.⁷ Organosolv produces a lignin fraction of high purity based on prior studies.¹⁵⁻¹⁷ Recently, a promising organosolv method was reported that affords lignin streams containing less than 0.5% residual sugar with yields as high as 97%.^{15, 18}

Understanding the structures of the individual components in organosolv lignin is essential to tailoring downstream conversion methodology.¹⁹⁻²² Lignin presents a particularly difficult analytical challenge due to its complex structural motifs.^{3, 5, 8, 11, 12, 23} Current analysis techniques, such as NMR, only provide average structural features of the bulk mixture.^{18, 24} Tandem mass spectrometry is a powerful tool for structural characterization of unknown compounds in complex mixtures.²⁵⁻²⁷ In this study, high performance liquid chromatography (HPLC) coupled with multiple-stage tandem mass spectrometry (MSⁿ) and collision-activated dissociation (CAD) was used to obtain structural information on compounds in an organosolv

switchgrass sample that has been previously analyzed via multiple quantum coherence-nuclear magnetic resonance (HMQC-NMR) methodology.^{18,28} In tandem mass spectrometric characterization of complex mixtures, ionization of all analytes without fragmentation is essential to ensure that the molecular weight information is retained and that each ion with a different m/z -value corresponds to an analyte molecule with a specific MW.^{29,30} Previous studies have shown that by using electrospray ionization (ESI) doped with sodium hydroxide, the production of the deprotonated molecule is facilitated to such an extent that all phenolic compounds only produce a deprotonated molecule without fragmentation.^{31,32} By combining this technique with high resolution mass measurements, elemental compositions can be assigned to each analyte.^{32,33} For structural analysis, MSⁿ coupled with collisionally activated dissociation (CAD) was utilized.³³⁻³⁷ The structures of deprotonated molecules derived from organosolv switchgrass were assigned based on comparison of their fragmentation patterns to those of deprotonated model compounds published^{31,32,38-40} earlier. HPLC was needed to separate isomeric and isobaric analytes within the mixture.³² To our knowledge, this is the first report of an in-depth structural analysis of an organosolv lignin sample by utilizing the HPLC/MSⁿ/high resolution approach.

EXPERIMENTAL

Materials

Ethyl ferulate, coniferyl aldehyde, sinapaldehyde, p-coumaric acid, ferulic acid, sinapic acid, vanillin, syringaldehyde, 4-hydroxybenzaldehyde, 2-ethoxy-3-(4-hydroxyphenyl)propanoic acid (all 98% purity), vanillic acid and 2-hydroxy-3-(4-hydroxyphenyl)propionic acid (97% purity), polydatin (95% purity), and ammonium formate (>99% purity) were purchased from

Sigma-Aldrich (St. Louis, MO). High-performance liquid chromatography/mass spectrometry (HPLC/MS) grade water and acetonitrile were purchased from Fisher Scientific (Pittsburgh, PA). All chemicals were used without prior purification.

Methyl ferulate, p-coumaric methyl ester, p-coumaric ethyl ester,⁴¹ guaiacylglycerol- β -guaiacylether [G(8-O-4)G], 1-(4-hydroxy-3-methoxyphenyl)-2-(2-methoxyphenoxy)ethanone [MPE], 3-hydroxy-1-(4-hydroxy-3-methoxyphenyl)-2-(2-methoxyphenoxy)propan-1-one [MPP],⁴² 4,4'-diallyl-2,2'-dimethoxy-1,1'-biphenyl [E(5-5)E], and the 3,3'-dimethoxy-5,6'-dimethyl-[1,1'-biphenyl]-2,2'-diol [MG(5-5)MG]⁴³ were synthesized using previously published procedures. Zorbax SB-Phenyl column (4.6 x 250 mm, 5 μ m particle size) was purchased from Agilent Technologies (Santa Clara, CA).

Organosolv switchgrass lignin was obtained by treating knife milled switchgrass (1-2" in length) in a flow through reactor with a 16:34:50 wt% mixture of methyl isobutyl ketone, ethanol, and water in the presence of a sulfuric acid (0.1 M) at a temperature of 120 °C for 56 min.¹⁸ The lignin was isolated from the resulting black liquor by mixing it with NaCl (10 g/ 100 mL) in a separatory funnel and allowed to separate into an aqueous phase containing hemicellulose degradation products and an organic layer containing lignin degradation products. The products of lignin degradation were isolated from the organic fraction through subsequent washes with water followed by rotary evaporation.

Sample Preparation

For CAD studies of deprotonated model compounds, stock solutions were prepared with a concentration of 1.0 mM in methanol/water 50/50 (v/v). For HPLC/MS analysis of the lignin fraction, the solid sample provided was dissolved in acetonitrile at 2 mg/mL. For direct injection

MS analysis of the lignin fraction, the solid sample provided was dissolved in acetonitrile at 4 mg/mL. 100 μ L of 1% sodium hydroxide solution (m/v) was then added to each mL of the prepared solution immediately before injection.

Instrumentation

All experiments were performed on a Thermo Scientific linear quadrupole ion trap (LQIT) / Fourier transform ion cyclotron resonance (FT-ICR; 7 Tesla magnet) mass spectrometer equipped with an ESI source. The instrument was operated using the LTQ Tune Plus interface and Xcalibur 2.1 software. The mass spectrometer was coupled to a Surveyor Plus high-performance liquid chromatograph with a quaternary pump, auto sampler, and photodiode array (PDA) detector. Samples analyzed by direct injection were introduced into the mass spectrometer via syringe drive at 15 μ L/min. To facilitate formation of a stable ESI spray, the sample was combined with methanol/water 50/50 (v/v) eluting from a Finnigan Surveyor MS Pump Plus at 200 μ L/min via a tee connector. The resulting mixture was introduced into the ESI source. For samples analyzed via HPLC/MS, the eluents of the column were mixed via tee connector with a 1% sodium hydroxide solution at a flow rate of 0.1 μ L/min. The ESI conditions were set as follows: 3.5 kV spray voltage, flow of 20 (arbitrary units) sheath gas, flow of 10 (arbitrary units) auxiliary gas, and a 275 C transfer capillary temperature. All ion optic voltages were set using the LTQ Tune Plus interfaces tuning features. The nominal pressure within the instrument, as read by the ion gauges, was maintained at 0.60×10^{-5} Torr in the LQIT and 2.0×10^{-10} Torr in the FT-ICR. In the determination of elemental compositions, a resolving power of 400,000 was used to achieve mass accuracies below 10 ppm.

High Performance Liquid Chromatography/Tandem Mass Spectrometry

For HPLC/MS analysis, all samples were introduced using an autosampler with a full-loop injection volume for high reproducibility. The mobile phase solvents used are a 0.001% (m/v) ammonium formate in water solution (A) and 0.001% (m/v) ammonium formate in acetonitrile solution (B). Ammonium formate is used as a buffer to encourage negative ion production. A non-linear gradient used is as follows: 0.00 minutes, 80% A and 20% B; 23.00 minutes, 25% A and 75% B; 24.00 minutes, 5% A and 95% B; 24.99 minutes, 5% A and 95% B; 25.00 minutes, 80% A and 20% B; 35.00 minutes, 80% A and 20% B. The column was located in a thermostatted compartment where the temperature was maintained at 30 C. Mass spectrometric analysis of the HPLC eluents was performed using the data dependent functionality of the Xcalibur software. Data dependent scans allow for several MSⁿ experiments to be carried out in the LQIT (higher duty cycle), while acquiring high-resolution spectra from the FT-ICR (lower duty cycle) at a resolving power of 400,000 at m/z 400. Data dependent acquisition of MSⁿ spectra involves the automatic selection of the most abundant ions in the LQIT to be subjected to isolation and fragmentation. Further, their most abundant fragment ions are selected for further isolation and fragmentation. For MSⁿ experiments, an isolation window of 2 m/z was used prior to ion fragmentation at a q value of 0.25 for 30 ms at a normalized collision energy of 35% (arbitrary units). All ionic fragmentation products of at least 5% relative abundance are reported within.

Extracted ion chromatograms (XICs) were produced via the Xcalibur 2.1 software. After separation, the elemental compositions of all ionized analytes were determined from high-resolution data acquired using the FT-ICR. Based on their elemental compositions, analytes were grouped into classes of compounds with distinguishing characteristics, such as a specific

carbon:oxygen (C:O) ratio, mass, and double bond equivalence (DBE). Using these data, XICs were obtained for each compound class via a data mining process wherein the total ion current of the selected ionized analytes is plotted as a function of HPLC retention time. Lists of the exact masses of the ionized analytes for each class were compiled. The XICs were obtained by entering these mass lists into the Xcalibur software under “Mass Range.” The software then plots the total ion current for the selected masses as a function of HPLC retention time. This process was repeated for each class of analytes.

RESULTS AND DISCUSSION

In order to characterize the main components of organosolv switchgrass, the sample was separated using reverse phase HPLC with a phenyl column. Upon elution, all ions generated upon ESI (via deprotonation of the analytes) were detected in the mass spectrometer. The most abundant ions formed from the ionized analytes were subjected to isolation and CAD experiments, and high-resolution mass spectra were measured to obtain their elemental compositions. Initial separation of the organosolv switchgrass sample (Figure 1) shows that the mixture is very complex. In an effort to diagnose the main components in the mixture, the high-resolution data were used to produce representative extracted ion chromatograms for each class of components present.

High Resolution Analysis of Organosolv Switchgrass Sample

High-resolution analysis via FT-ICR allows the determination of the elemental compositions of all ionized analytes present in the organosolv switchgrass sample. Based on the elemental compositions, distinct characteristics of the analytes can be determined. For this study,

C:O ratios, DBEs, and molecular weights were used to group the analytes in the mixture into distinct categories. For example, the C:O ratio can be used to determine whether the analyte is a carbohydrate (lower C:O ratio) or lignin related (higher C:O) ratio. The DBE is indicative of the degree of saturation and correlates with the amount of aromatic rings (DBE of 4) and double bonds (DBE of 1) in the molecule. Finally, the molecular weight correlates with the number of monomers in the analyte.

Using above traits, three groups of analytes were identified: low molecular weight analytes (including monomeric lignin related compounds, fatty acids, and monosaccharides), dimeric lignin related analytes, and lignin-carbohydrate complexes. The ion current produced by the analytes in each class during an HPLC run (extracted ion chromatograms) represent the contribution of each class to the total ion current. Figures 1A, 1B, and 1C show the normalized extracted ion chromatographs (XICs) for all three classes. The lignin monomers are identified based on their low molecular weights and higher DBE values than for monosaccharides and fatty acids. The DBE values for the monomers range from 5 to 6. DBEs of 4 or higher are indicative of an aromatic ring and the low molecular weight indicates that this is a small aromatic analyte. In addition, the C:O ratio is $\geq 5:2$ for all of the monomeric lignin analytes. The monomeric analytes primarily have HPLC elution times between 10-20 minutes (Figure 1A). In addition, fatty acids and monosaccharides were identified in this class based on their elemental compositions and low DBE values (Table S1).

The same approach was used to identify the dimeric lignin analytes. The elemental compositions reveal DBE values higher than 8 (indicative of two aromatic rings), the same C:O ratios as for monomeric lignin compounds, and higher molecular weights to account for the additional monomer unit. After extraction of the ion current produced by these analytes during

an HPLC run, it can be concluded that the dimeric lignin analytes take 10-22 minutes to elute from the column (Figure 1B). Finally, this methodology was used to identify lignin-carbohydrate complexes in the mixture. The molecular weights of these analytes indicate that they are dimeric lignin compounds, however, their lower DBEs indicate that they contain a saturated ring (sugar moiety) (Table 2). In addition, the C:O ratio is too low for purely aromatic lignin analytes, $\leq 2:1$. Figure 1C shows the XIC resulting from lignin-carbohydrate complexes.

To study the relative ionization efficiencies of the different analyte types in organosolv lignin, an equimolar mixture of four model compounds, vanillin, polydatin, guaiacylglycerol- β -guaiacylether, and MG(5-5)MG (Figure 2) was studied. The equimolar mixture was directly injected into the ESI source after being doped with NaOH solution. Figure 2 suggests no bias for any components in this mixture. Since each of the analytes gets ionized almost equally efficiently without fragmentation, semi-quantitative information is obtained without internal standards. By normalizing chromatograms A, B, and C in Figure 1, it is clear that the major products are lignin-carbohydrate complexes (possibly from the cell walls), followed by monomers and then dimers. We demonstrated this to be a correct statement by spiking the organosolv lignin sample with a tetrameric model compound at a concentration of 0.1 mM and analyzing this mixture by using HPLC/tandem mass spectrometry. We were easily able to detect the model compound in the mixture (Figure S1). Since the only major lignin derived products observed are monomers and dimers, the organosolv process used can be concluded to greatly degrade the lignin polymer and extract lignin carbohydrate complexes from the cell wall. However, further structural understanding of the resulting products is desired. To be able to elucidate the structures of these analytes, ionized model compounds were studied to better understand the fragmentation of the ionized unknown analytes in the organosolv mixture.

Dissociation Reactions of Deprotonated Monomeric Model Compounds

In order to explore the type of structural information that can be obtained from dissociation reactions of different ionized lignin degradation products, several deprotonated monomeric model compounds were subjected to CAD (Table 1). Deprotonated 4-hydroxybenzaldehyde loses small neutral molecules of MW of 28 and 29 Da upon CAD, corresponding to the formation of $[M-H-CO]^-$ and $[M-H-COH]^-$, respectively. Both reactions likely involve the cleavage of the benzene-aldehyde carbon-carbon bond and they facilitate the identification of the aldehyde functionality. For the deprotonated methoxy substituted benzaldehydes, vanillin and syringaldehyde, the loss of a methyl radical was observed to be indicative of a methoxy group (if necessary, MS^4 can be used to identify the presence of the carbonyl group although the data are not shown here). Deprotonated vanillin shows unique behavior as it exhibits loss of a molecule with MW of 44 Da to generate $[M-H-CO_2]^-$ (Table S2). The mechanism of this reaction is under investigation.

In an effort to focus on more relevant analytes, several model compounds were studied that are derivatives of sinapyl and coniferyl alcohol, the building blocks of lignin (Table 1). These compounds include, for example, sinapaldehyde and coniferaldehyde. After deprotonation and CAD, they exhibit methyl radical losses from the methoxy substituents on the ring, as expected. When the resulting fragment ions were isolated and subjected to CAD, the losses of CO and COH were observed (Table 1), as also seen for deprotonated 4-hydroxybenzaldehyde. In addition, C_3H_4O (possibly 2-propenal) was lost from deprotonated coniferaldehyde after a

methyl radical was lost. Based on the loss of C_3H_4O , the number of carbons in the aldehyde moiety can be determined.

In addition to aldehydes, the acid derivatives of coniferyl and sinapyl alcohols, *i.e.*, coumaric and ferulic acids, were studied. Each deprotonated analyte exhibits the loss of CO_2 upon CAD, indicative of the presence of a carboxylic acid functionality. When a methoxy is present on the ring, as for ferulic acid, CO_2 and a methyl radical are lost in succession. The same fragmentation pathways were observed for deprotonated vanillic acid. To complement the study of ferulic, coumaric, and vanillic acids, another similar analyte with an additional hydroxyl group, 2-hydroxy-3-(4-hydroxyphenyl)propionic acid, was studied. This deprotonated analyte loses water from the alcohol group, as expected. However, it did not exhibit the loss of CO_2 as seen for other deprotonated carboxylic acids. Instead, loss of a molecule with MW of 46 Da (likely $HCOOH$) was observed. This loss has not been observed for other deprotonated monomeric lignin model compounds.^{31, 32, 39, 40}

Due to the inherent use of methanol or ethanol in organosolv lignin extraction, CAD of deprotonated methyl and ethyl esters of ferulic and coumaric acids was studied to account for possible esterification of analytes during the isolation process. Their fragmentation was compared to that of their isomers, deprotonated sinapaldehyde and coniferaldehyde, respectively. Deprotonated coniferaldehyde and coumaric methyl ester can be distinguished due to the fragment ions $[M-H-CH_3OH]^-$ and $[M-H-CH_3-CO_2]^-$ that are produced upon CAD of only the deprotonated coumaric methyl ester (Scheme 1), in addition to the loss of a methyl radical. Deprotonated coniferaldehyde only loses a methyl radical. However, further isolation of fragment ions and CAD (MS^3) is required to distinguish deprotonated sinapaldehyde and ferulic methyl ester isomers, which only produce an ion of m/z 207 upon CAD via the loss of a methyl

radical. After isolation of the fragment ions of m/z 207 and subjection to collisional activation, differing fragmentation was observed for the two isomers. The ion of m/z 207 derived from sinapaldehyde shows loss of a methyl radical from the second methoxy group while the ion derived from ferulic methyl ester exhibits losses of a methyl radical and CO_2 in succession.

Based on the study of the two methyl esters, the methyl radical must be lost from the ester substituent before the loss of CO_2 takes place. This fragmentation pattern is unique to the ester functional group and is essential for distinction of the isomers discussed above. For the corresponding ethyl esters, analogous losses were observed, including $\text{CH}_3\text{CH}_2\text{OH}$ and CH_2CH_2 losses followed by the loss of CO_2 (Scheme 2).

In addition to esters, an ethyl ether analog, 2-ethoxy-3-(4-hydroxyphenyl)propanoic acid, was studied. This deprotonated ethyl ether fragments via exclusive loss of ethanol. It is proposed that ferulic acid is formed upon loss of ethanol (Scheme 3). In addition, this mechanism can be applied to the loss of water from 2-hydroxy-3-(4-hydroxyphenyl)propanoic acid. This is further supported by the loss of CO_2 upon further isolation and CAD of the resulting fragment ion. This finding indicates that the loss of ethanol is more facile than the loss of CO_2 . This clean loss of ethanol is unusual for lignin model compounds. In conclusion, the fragmentation of the deprotonated monomeric analytes displays predictable pathways that can be used to propose structures for unknown lignin related analytes in biomass mixtures.

Structural Elucidation of Monomeric Compounds in Organosolv Lignin

Figure 3 shows the XIC measured for an HPLC/MS run of organosolv lignin for the class of the low molecular weight analytes. Based on the accurate mass analysis, the analytes that elute at ~3 minutes are carbohydrates due to their low C:O ratio, $\leq 2:1$. This is not unexpected since the organosolv procedure may leave residual carbohydrates in the lignin fraction.^{15, 18} Negative-ion mode ESI doped with NaOH is not suited for carbohydrate analytes since after deprotonation, they readily lose water, yielding two types of ions, $[M-H]^-$ and $[M-H_2O]^-$, for each carbohydrate. Fatty acids were observed later in the HPLC run (>27 min). These deprotonated analytes are readily identified due to their elemental compositions indicating a long hydrocarbon chain with up to 15 carbons and two oxygens (Table S1).

Based on above model compound studies (Table 1), several analytes can be readily identified in the organosolv lignin sample. For monomeric analytes, deprotonated compounds A_{1-10} (Figure 3) have fragmentation patterns (Table S4) and elemental compositions (Table 2) that are identical to some of the ionized model compounds studied (Table 1). When comparing the unknown analytes to the model compounds studied, the relative abundances of the fragment ions measured in each stage of CAD (MS^2 and MS^3) were compared. The relative abundances of the ionized unknown A_{1-10} analytes' fragment ions differed less than 3% from the relative abundances measured for the ionized model compounds' fragment ions. Therefore, the structures of the unknown analytes can be assigned with confidence. The majority of the analytes identified are derivatives of coniferyl and sinapyl alcohol. For example, ethyl ferulate and ethyl coumarate were identified. These compounds are present due to the use of ethanol for the extraction of lignin.¹⁸ The remaining identified analytes correspond to lignin monomers with aldehyde and acid functionalities. An additional monomeric structure (A_{10}) is proposed for one of the

deprotonated compounds in the sample based on the observed fragmentation and measured elemental composition (Table 4). Upon CAD, the deprotonated analyte exhibits the loss of H, COH, and CH₃. Based on the model compound studied here (Table 1), the analyte is not a simple aldehyde with a methoxy group since CH₃ is not the only loss upon CAD in MS². The loss of COH in combination with CH₃ supports the presence of a hydroxyl group on the side chain (Table 4).

Dissociation Reactions of Deprotonated Dimeric Model Compounds

The dissociation reactions of many deprotonated dimeric lignin model compounds have been explored by Morreel *et al.*^{39,40} These analytes include β -aryl ethers, phenylcoumarans, and resinols containing common linkages, such as β -O-4, β -5, and β - β . The deprotonated analytes were demonstrated to be easy to identify based on their unique fragmentation patterns. The losses of diagnostic neutral molecules with specific branching ratios were used to diagnose the type of lignin linkage present in the analytes.^{39,40} For example, the deprotonated resinol dimer G(β - β)G containing the β - β linkage primarily lost the A unit (Table S3). In addition, the characteristic loss of a molecule with MW of 46 Da (HCOOH) was observed with 15% relative abundance. This loss, in combination with the loss of the A unit, allows for the identification of the β - β linkage present in this dimer.⁴⁰

Morreel *et al.*^{39,40} also examined CAD of a deprotonated resinol dimer G(β - β)FA (Table S3). This deprotonated analyte exclusively exhibited the loss of CO₂. This is unique fragmentation that has not been observed for other deprotonated dimeric lignin model compounds. On the other hand, the deprotonated phenylcoumaran dimer, G(β -5)G (Table S3), yielded only one fragment ion, [M-H-A]⁻ (Table S3). The presence of a single fragment ion

resulting from cleavage of the dimer linkage is unique to the phenylcoumarin dimer. Finally, Moreel *et al.* found that a deprotonated β -aryl ether, G(β -O-4)G, predominately exhibits the characteristic losses of H₂O and CH₂O resulting in the net loss of 48 Da to produce the fragment ion [M-H-H₂O-CH₂O]⁻ (Table S3). This fragment ion was shown to be unique to β -O-4 dimers.

However, the study by Moreel *et al.* only addressed lignin dimers with common linkages. To account for degradation or modification of the linkages in the molecules during the extraction process and to address the possible presence of additional linkages proposed in the literature,⁴⁴⁻⁴⁶ new lignin dimers were synthesized to study their fragmentation pathways after deprotonation. For example, deprotonated dimers with 5-5 linkages and oxidized β -O-4 linkages (containing an α -keto functionality; Table 3) were studied to provide a more inclusive CAD dataset. Instead of undergoing fragmentation at the linkage, ions containing the 5-5 linkage only undergo fragmentation in their functional groups. For example, deprotonated MG(5-5)MG (Table 3) exclusively loses a CH₃ radical. This is unique fragmentation behavior that has not been observed for related deprotonated dimeric model compounds. The strength of the 5-5 linkage prevents its cleavage, unlike all other linkages studied thus far.^{39,40} Hence, 5-5 linkages can be identified based on the lack of cleavage of the linkage. Isolation of the fragment ion formed upon methyl radical loss from deprotonated MG(5-5)MG and subjection to CAD resulted in another CH₃ radical loss, followed by losses of H₂O and COH. The loss of H₂O was unexpected for this analyte since this loss has primarily been observed for deprotonated aliphatic alcohols, such as sinapyl alcohol.^{31,32} Similar fragmentation was observed for a deprotonated eugenol dimer with a 5-5 linkage, (E(5-5)E) (Table 3). The fragment ion formed upon CH₃ loss was isolated and subjected to CAD (MS³ experiment). Several structurally diagnostic fragment ions were observed, including [M-H-H]⁻, [M-H-CH₃]⁻, [M-H-H₂O]⁻, and [M-H-C₃H₅]⁻ (Table 3).

Observation of the loss of a CH_3 radical from the second methoxy group shows that by using consecutive CAD events, the methoxy substituents on deprotonated 5-5-linked dimers can be counted. Another characteristic fragmentation for the deprotonated dimers containing a 5-5 linkage is the loss of H_2O from a fragment ion that has lost all readily cleavable groups, such as CH_3 groups from all methoxy groups (Table 3).

In addition to the ability to identify the 5-5 linkage in dimers, structural information can be obtained on the functional groups in these dimers. For example, after a loss of CH_3 from deprotonated E(5-5)E, a hydrogen atom is lost via cleavage of a benzylic carbon–hydrogen bond (Table 3), which was seen for deprotonated monomeric eugenol in previous studies.³¹ Additional structural information for deprotonated E(5-5)E can be obtained from the fragment ion $[\text{M}-\text{H}-\text{C}_3\text{H}_5]^-$. The presence of the 5-5 linkage allows for the loss of the propenyl radical due to increased conjugation in the molecule compared to monomeric eugenol. This fragmentation has not been observed for deprotonated monomeric eugenol.

CAD of deprotonated model compounds with an oxidized β -O-4 linkage was also explored (MPE and MPP, Table 3). Instead of an α -hydroxy functionality, MPE and MPP contain a keto functionality in the α position. The deprotonated model compounds show unique fragmentation behavior. While the fastest fragmentation reaction for deprotonated MPP is CH_3 loss, as seen for the deprotonated dimers with a 5-5 linkage, it is accompanied by a slow cleavage of the dimer linkage to lose B (guaiacyl unit) (Table 3). When the fragment ion $[\text{M}-\text{H}-\text{CH}_3]^-$ was isolated and subjected to CAD (Table 3), it was found to undergo benzylic cleavage of the dimer linkage. Addition of a hydroxymethyl group to the dimer linkage, as in MPE (Table 3), results in the formation of new fragment ions for the deprotonated molecule. As with MPP, deprotonated MPE undergoes a benzylic bond cleavage of the dimer linkage to lose a guaiacyl

unit, producing the fragment ion $[M-H-B]^-$. In addition, the fragment ion $[M-H-B-H]^-$ was observed for MPE (Table 3). However, the cleavage of the linkage occurs more readily for MPP than for MPE. Further, while deprotonated MPP loses a CH_3 radical, deprotonated MPE loses the hydroxymethyl group as CH_2O . It is clear that each deprotonated dimer has distinct fragmentation pathways that not only allow for the identification of the linkage but also some functional groups, such as carbonyl, hydroxyl, and alkene moieties.

Structural Elucidation of Dimeric Compounds in Organosolv Lignin

One of the dimeric compounds (unknown labeled as B_6 in Table S4) detected in the organosolv lignin sample (Figure 4) was identified to have the same structure as the G(β -5)FA model compound based on their deprotonated molecules' CAD (Table S3). Structures are proposed for the other abundant dimeric analytes in the organosolv lignin sample based on their deprotonated molecules' measured elemental compositions (Figure 4) and fragmentation pathways in combination with the knowledge acquired on the fragmentations of the deprotonated model compounds studied.

Compounds B_1 , B_2 , B_3 , B_4 , B_5 , and B_7 (Figure 4) were identified as 5-5 linked dimers due to the preservation of the dimer linkage upon CAD of the deprotonated molecules (Table 4). Based on the study of model compounds, this only occurs for 5-5 linked dimers (Table 3). Deprotonated B_3 , B_5 , and B_7 show only a facile loss of a CH_3 radical. After CH_3 loss, H_2O loss was observed in MS^3 experiments (Table 4). Deprotonated B_5 exhibits loss of C_3H_7O after CH_3 loss (Table 4). Based on the examination of deprotonated E(5-5)E model compound (Table 3), where the phenyl-carbon bond is cleaved to produce $\bullet C_3H_5$ ($CH_2=CH-CH_2\bullet$, *i.e.*, the allyl

radical) from a propenyl group, the loss of $\bullet\text{C}_3\text{H}_7\text{O}$ likely corresponds to loss of the $\text{HOCH}=\text{CH}-\text{CH}_2\bullet$ radical due to a phenyl-carbon bond cleavage.

Upon CAD of deprotonated B_4 (Table 4), ethanol loss was observed. Based on the fragmentation of the deprotonated monomeric model compound 2-ethoxy-3-(4-hydroxyphenyl)propanoic acid (Table 1), an ethyl ether is expected to readily lose ethanol. In addition, since no losses of CH_3 were observed, it can be concluded that analyte B_4 does not contain methoxy groups. Based on these findings, a 5-5 dimer with a benzylic ethyl ether moiety is proposed for analyte B_4 .

Deprotonated B_1 exhibits losses of several different neutral molecules upon CAD (Table 4). The most characteristic one is the loss of HCOOH . For deprotonated model compounds, this loss was only observed for the deprotonated resinol dimer, $\text{G}(\beta\text{-}\beta)\text{G}$, and deprotonated 2-hydroxy-3-(4-hydroxyphenyl)propanoic acid (Table 1). Further, CAD of deprotonated B_1 does not result in losses of large molecules, such as the loss of guaiacol unit from deprotonated $\text{G}(\beta\text{-}\text{O-}4)\text{G}$. The absence of large molecule losses indicates that B_1 does not contain weak linkages between the monomers, such as $\beta\text{-}\text{O-}4$, $\beta\text{-}\beta$, or $\beta\text{-}5$ (Table S3). Instead, a 5-5 linkage is likely to be present, together with a 2-hydroxy-3-(4-hydroxyphenyl)propanoic acid moiety. Based on these observations, the structure shown in Table 4 is proposed for B_1 . When the fragment ion formed upon HCOOH loss was isolated and subjected to CAD, loss of CO_2 was observed. This fragmentation sequence, loss of HCOOH followed by loss of CO_2 from deprotonated B_1 , supports the structure proposed (Table 4) as this sequence of losses was observed for deprotonated 2-hydroxy-3-(4-hydroxyphenyl)propanoic acid (Table 1).

The deprotonated unknown analyte B_2 (Table 4) does not show cleavage of the dimer linkage, just as was observed for deprotonated B_1 , and hence is likely to contain the 5-5 linkage.

CAD of deprotonated B₂ involves predominant loss of CH₂O. This loss has been observed only for deprotonated dimeric model compounds with β-O-4 linkages. However, since B₂ is likely to contain the 5-5 linkage, the loss of CH₂O must originate from a different moiety than the β-O-4 linkage. The DBE and C:O ratio for deprotonated B₂ are abnormally high at 16 and 23:3, respectively. Due to these values, it is apparent that this molecule has a high degree of unsaturation and very few oxygens (Table 4). Hence, the structure shown in Table 4 is proposed for B₂.

Finally, fragmentation of deprotonated B₈ mimics the fragmentation of deprotonated MPE and MPP model compounds (Table 3). However, deprotonated B₈ also exhibits loss of CO₂, indicative of a carboxylic acid functionality. A methoxy substituent must also be present due to the competitive losses of a CH₃ radical and CO₂. Isolation and CAD of the fragment ion produced upon the loss of CO₂ from deprotonated B₈ involves the loss of a CH₃ radical, further supporting the presence of a methoxy group in the ion. Hence, a structure containing an α-keto functionality, methoxy substituent and a carboxylic acid substituent is proposed for B₈ (Table 4).

For deprotonated lignin-carbohydrate dimers, unique fragmentation patterns were observed. Based on the elemental compositions of these analytes, it is proposed that there is a coumaric acid moiety linked to a carbohydrate (Table 2). For deprotonated C₁ and C₃ (Table 4), the major fragmentation pathway involves the loss of C₂H₄O₂. This loss is attributed to the cleavage of the ring in the sugar moiety.⁴⁷ This loss was not observed for the deprotonated lignin related molecules discussed above. For C₁ and C₃, isolation and CAD of the fragment ion resulting from C₂H₄O₂ loss leads to C₃H₄O₂ loss. This loss likely involves the cleavage of the carbon-oxygen bond linking the coumaric acid moiety to the carbohydrate moiety. Deprotonated C₁ and C₃ show the same fragmentation pathways, indicating that they have the same base

structure. However, deprotonated C_3 has 30 units greater m/z -value indicating that it has an additional methoxy group on the aromatic ring. Based on these observations, the structures shown in Table 4 were assigned to C_1 and C_3 .

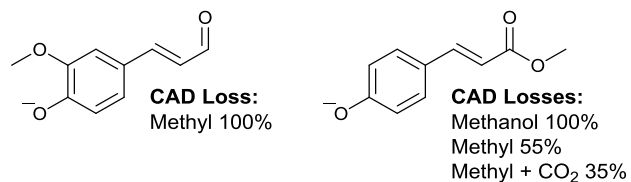
Deprotonated C_2 and C_4 show similar fragmentation pathways to each other but differ in their m/z -values by the mass of a methoxy group. Upon CAD, both deprotonated C_2 and C_4 show the loss of the entire carbohydrate moiety ($C_7H_{14}O_4$). It is proposed that this occurs similarly to the loss of methanol from the coumaric methyl ester (Table 1) by cleavage of the carbon-oxygen bond at the α -position relative to the carbonyl group followed by consecutive water loss. For deprotonated C_4 , loss of a CH_3 radical was also observed. This is attributed to the presence of a methoxy group on the aromatic ring. Further CAD of the $[M-H-C_7H_{14}O_5]^-$ fragment ion formed from deprotonated C_4 only proceeds via the loss of a CH_3 radical. Upon CAD of the $[M-H-C_7H_{14}O_5]^-$ fragment ion of deprotonated C_2 , the loss of CO was observed, indicative of the presence of a hydroxy group on the ring for the lignin portion of the analyte. Despite differences in fragmentation pathways between the two pairs, deprotonated C_1/C_3 and C_2/C_4 , conclusions cannot be made about the exact structure of their carbohydrate moieties since they are lost in the first CAD event. The only observable difference between C_1/C_3 and C_2/C_4 analytes is the size of the carbohydrate moiety. The loss of a large neutral molecule with a higher C:O ratio than expected for lignin analytes is characteristic of this class of compounds and can be used to identify lignin-carbohydrate dimers in complex mixtures (Figure 5).

CONCLUSIONS

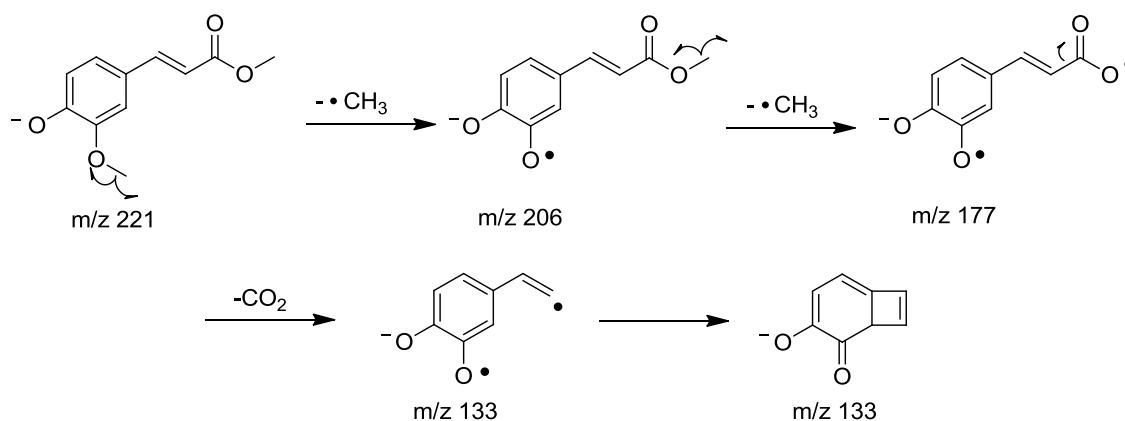
By combining HPLC separation with powerful high-resolution tandem mass spectrometry involving the measurement of elemental compositions and determination of analyte classes as well as gathering in-depth structural information from MS^n /CAD experiments, allows thorough molecular-level

characterization of unknown mixtures derived from degraded lignin. This was demonstrated by identifying the major products in an organosolv switchgrass sample. In further support of the proposed structures, many of them are in agreement with the presence of specific functionalities obtained using NMR techniques for the same sample.¹⁸ However, this study revealed that the functionalities identified by NMR are present in small molecules instead of polymers, as expected.^{18,46} Indeed, this study shows that native lignin degrades excessively during the organosolv extraction process. Only strong linkages, such as in 5-5, survived the process. Furthermore, no hydroxyl groups were identified in the degradation products while aldehyde and carboxylic acid functionalities were found to be common. The deviation of these results from earlier GPC analyses of the molecular weight distributions of compounds in organosolv lignins is likely due to a lack of suitable standards needed to calibrate GPC measurements as well as the strong tendency of lignins to form aggregates in solution.⁴⁸ As opposed to GPC, mass spectrometry measures directly the masses of the ionized molecules. Furthermore, we have used known, synthesized model compounds and their mixtures to demonstrate that our mass spectrometric measurements are able to reveal the real MWs of lignin type molecules.

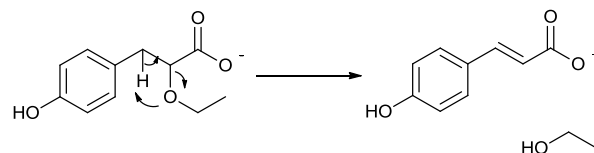
Tables and Figures



Scheme 1. The major fragmentations upon CAD for isomeric ions of m/z 177, deprotonated 4-hydroxy-3-methoxycinnamaldehyde and methyl coumarate.



Scheme 2. Proposed collision-activated dissociation pathway for the loss of a methyl radical followed by loss of carbon dioxide from deprotonated methyl ferulate.



Scheme 3. Proposed collision-activated dissociation pathway for the loss of ethanol from deprotonated 2-ethoxy-3-(4-hydroxyphenyl)propanoic acid.

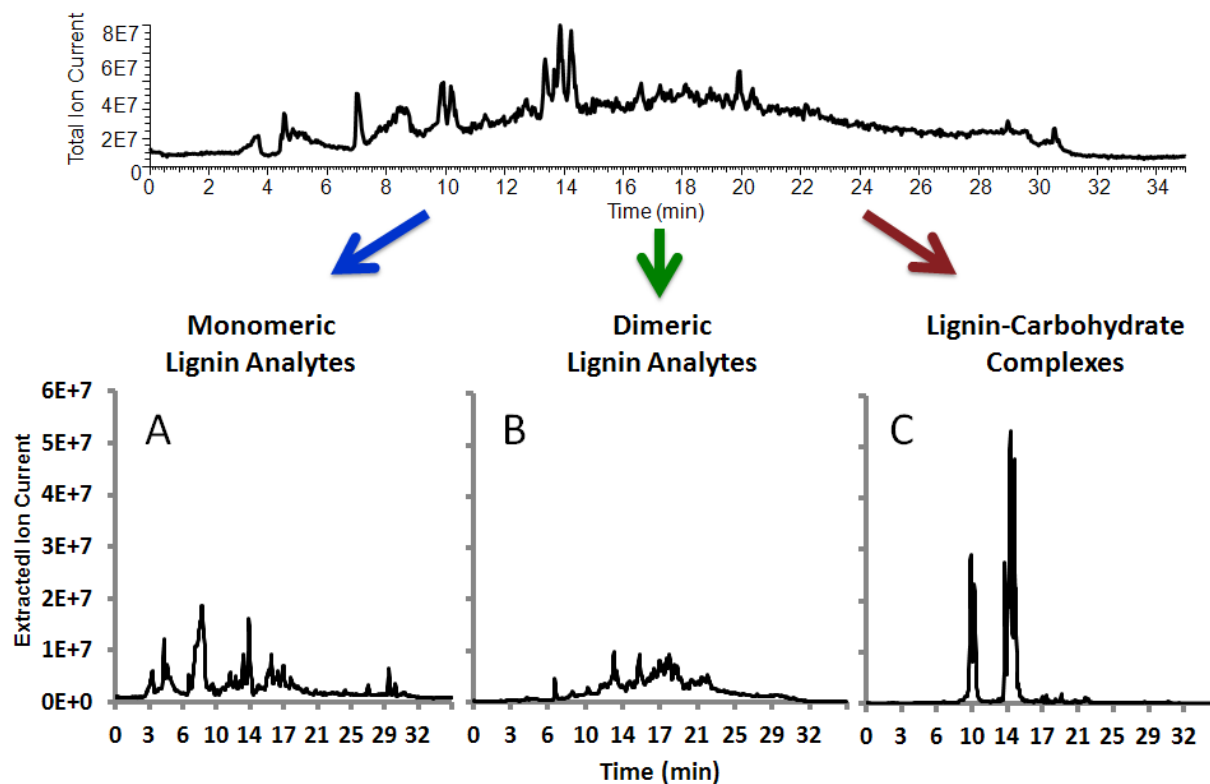


Figure 1. Top: HPLC total ion chromatogram obtained using ESI in the negative-ion mode for organosolv switchgrass mixture. Bottom: **A:** Extracted ion chromatogram for deprotonated analytes with C:O ratios $\geq 5:2$, m/z values from 90 up to 250, and double bond equivalence from 4 up to 7. **B:** Extracted ion chromatogram for deprotonated analytes with C:O ratios $\geq 5:2$, m/z values from 250 up to 400, and double bond equivalence > 8 . **C:** Extracted ion chromatogram for deprotonated analytes with C:O ratios $\leq 2:1$, m/z values from 250 up to 400, and double bond equivalence ≤ 6 . The ion current for additional low molecular weight analytes are also shown, including fatty acids and monosaccharides.

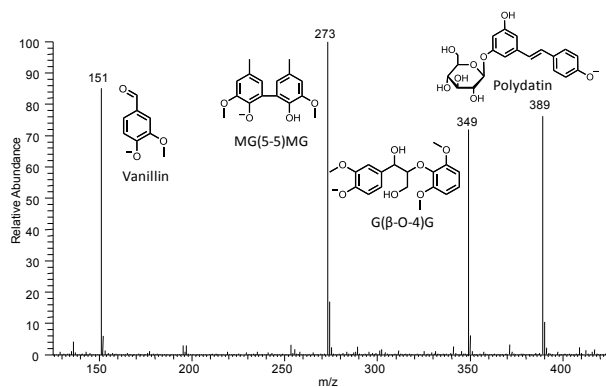


Figure 2. Negative ion-mode ESI mass spectrum obtained for an equimolar mixture of vanillin (MW 152 Da), MG(5-5)MG (MW 274 Da), G(β -O-4)G (MW 350 Da), and polydatin (MW 390 Da) dissolved in 50/50 (v/v) methanol/water and doped with sodium hydroxide.

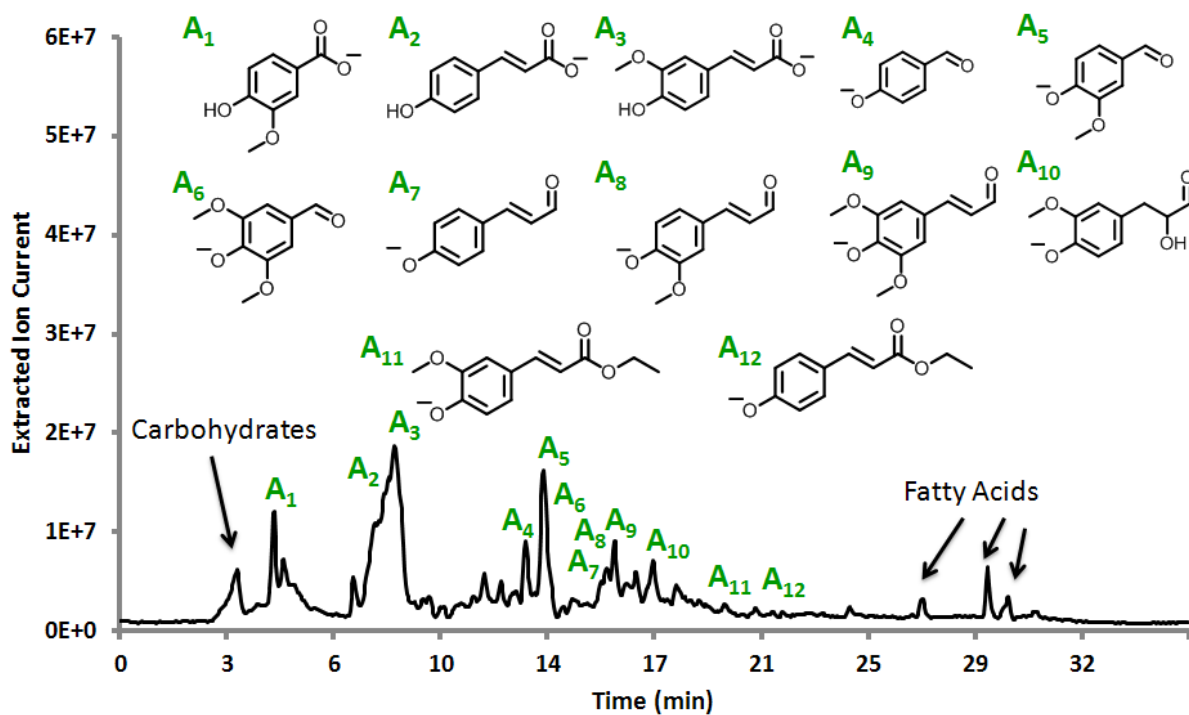


Figure 3. Selected ion HPLC chromatogram extracted from HPLC/ESI negative-ion mode total ion current for low molecular weight analytes, including sugars, fatty acids, and monomeric lignin related analytes.

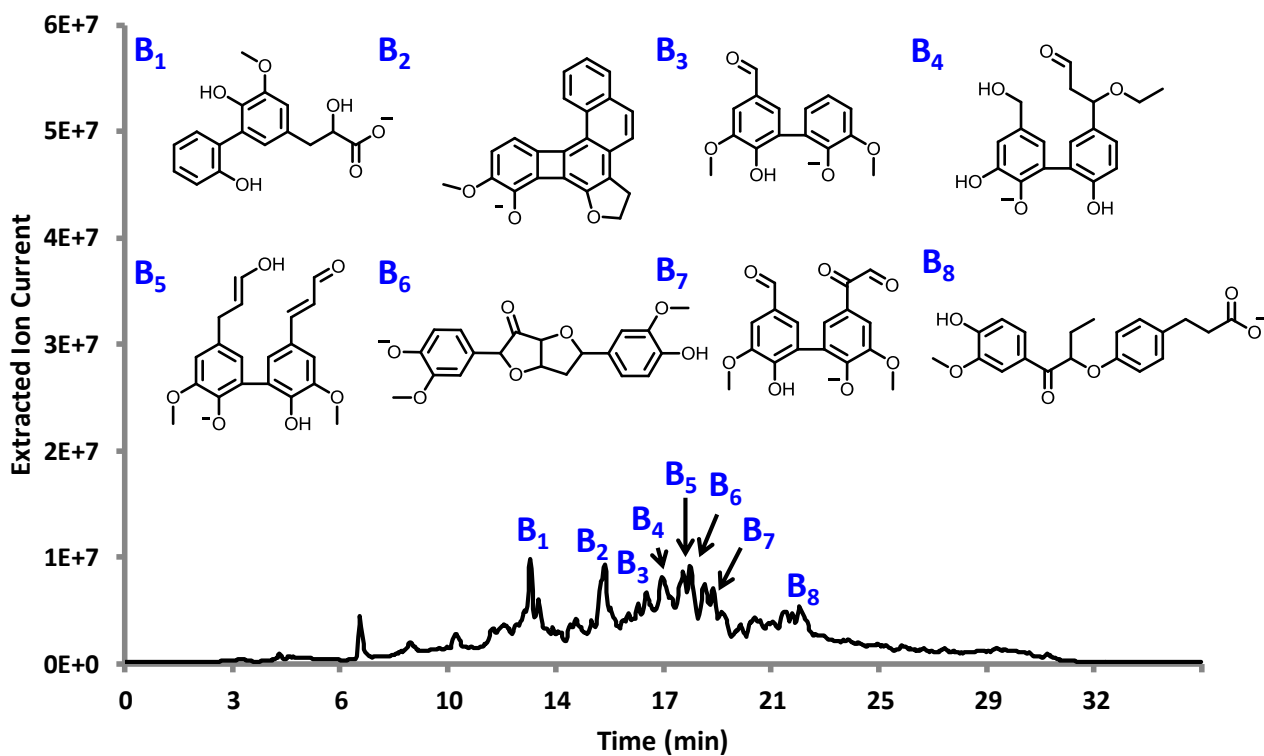


Figure 4. Selected ion HPLC chromatogram extracted from HPLC/ESI negative-ion mode total ion current for dimeric lignin related analytes.

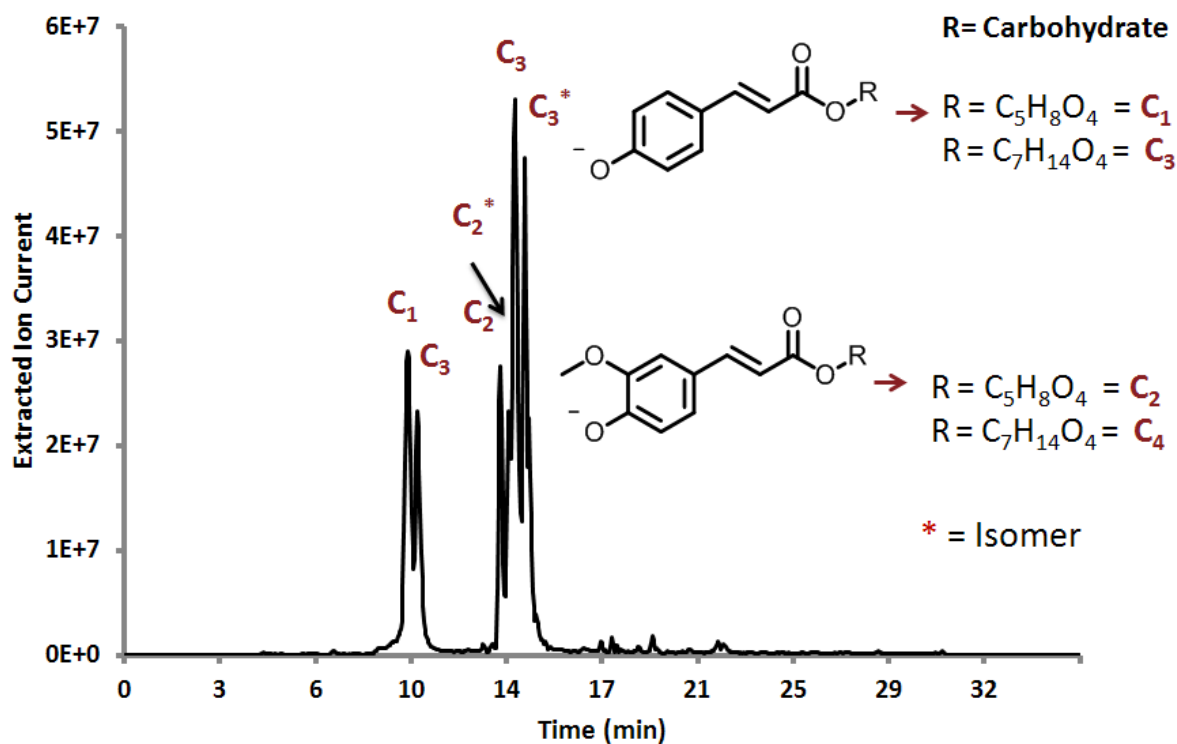
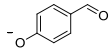
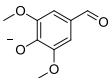
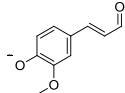
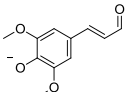
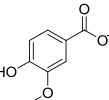
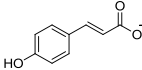
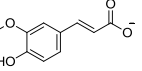
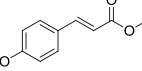
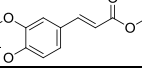
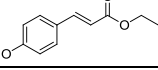
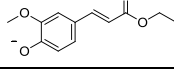
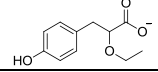
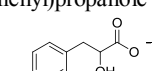


Figure 5. Selected ion HPLC chromatogram extracted from HPLC/ESI negative-ion mode total ion current for lignin-carbohydrate complexes.

Table 1. Deprotonated molecules formed upon negative-ion mode ESI from monomeric lignin model compounds, and the fragment ions of the deprotonated molecules with their relative abundances, and the fragment ions' fragment ions with their relative abundances, formed in consecutive ion isolation/CAD experiments.^a

Model Compounds (m/z of [M-H] ⁻)	MS ² /CAD Product Ions (m/z) and Their Relative Abundances	MS ³ /CAD Product Ions ^a (m/z) and Their Relative Abundances
4-Hydroxybenzaldehyde (121) 	121-CO (93) 100% 121-COH (92) 22%	93: No further fragmentation
Syringaldehyde (181) 	181-CH ₃ (166) 100%	166-CH ₃ (151) 100%
Coniferaldehyde (177) 	177-CH ₃ (162) 100%	162-CO (134) 100% 162-COH (133) 33% 162-C ₃ H ₄ O (106) 12%
Sinapaldehyde (207) 	207-CH ₃ (192) 100%	192-CH ₃ (162) 100%
Vanillic acid (167) 	167-CH ₃ (152) 100% 167-CO ₂ (123) 47%	152-CO ₂ (108) 100%
Coumaric acid (163) 	163-CO ₂ (119) 100%	119: No further fragmentation
Ferulic acid (193) 	193-CH ₃ -CO ₂ (134) 100% 193-CO ₂ (149) 42% 193-CH ₃ (178) 8%	134: No further fragmentation
Coumaric methyl ester (177) 	177-CH ₃ OH (145) 100% 177-CH ₃ (162) 55% 177-CH ₃ -CO ₂ (118) 35%	145-CO (117) 100%
Ferulic methyl ester (207) 	207-CH ₃ (192) 100%	192-CH ₃ (177) 100% 192-CH ₃ -CO ₂ (133) 24% 192-CO (164) 10%
Coumaric ethyl ester (191) 	191-C ₂ H ₄ (163) 100% 191-C ₂ H ₆ O (145) 22% 191-C ₂ H ₄ -CO ₂ (119) 13% 191-C ₂ H ₅ (162) 8%	163-CO ₂ (119) 100%
Ferulic ethyl ester (221) 	221-CH ₃ (206) 100%	206-C ₂ H ₅ (177) 100% 206-C ₂ H ₅ -CO ₂ (133) 35% 206-C ₂ H ₄ (178) 25% 206-C ₂ H ₄ -CO ₂ (134) 8%
2-Ethoxy-3-(4-hydroxyphenyl)propanoic acid (209) 	209-C ₂ H ₆ O (163) 100%	163-CO ₂ (119) 100%
2-Hydroxy-3-(4-hydroxyphenyl)propanoic acid 	181-H ₂ O (163) 100% 181-HCOOH (135) 10%	163-CO ₂ (119) 100%

^a MS³ was performed only for the most abundant product ion in the MS² spectra to avoid sacrificing the duty cycle of the instrument.

Table 2. Elemental compositions obtained from exact mass measurements for the deprotonated major components in the organosolv switchgrass sample (Figure 1). The errors for the exact mass measurements are reported in \pm milli mass units.

m/z of [M-H] ⁻ ; Determined Elemental Composition	Proposed Structure	Measured Exact m/z (Error \pm mmu From Expected Mass)	Double Bond Equivalence of Neutral Molecule
A ₁ : 167; C ₈ H ₇ O ₄		167.0365 (1.4)	5
A ₂ : 163; C ₉ H ₇ O ₃		163.0404 (1.4)	6
A ₃ : 193; C ₁₀ H ₉ O ₄		193.0509 (1.4)	6
A ₄ : 121; C ₇ H ₅ O ₂		121.0300 (1.5)	5
A ₅ : 151; C ₈ H ₇ O ₃		151.0404 (1.4)	5
A ₆ : 181; C ₉ H ₉ O ₄		181.0509 (1.4)	5
A ₇ : 147; C ₉ H ₇ O ₂		147.0455 (1.5)	6
A ₈ : 177; C ₁₀ H ₉ O ₃		177.0560 (1.4)	6
A ₉ : 207; C ₁₁ H ₁₁ O ₄		207.0664 (1.4)	6
A ₁₀ : 193; C ₁₀ H ₉ O ₄		193.0545 (1.4)	6
A ₁₁ : 191; C ₁₁ H ₁₁ O ₃		191.0716 (1.3)	6
A ₁₂ : 221; C ₁₂ H ₁₃ O ₄		221.0822 (1.3)	6
B ₁ : 303; C ₁₆ H ₁₅ O ₆		303.0877(1.3)	9
B ₂ : 339; C ₂₃ H ₁₅ O ₃		339.0992 (1.4)	16
B ₃ : 273; C ₁₅ H ₁₃ O ₅		273.0772 (1.4)	9
B ₄ : 331; C ₁₈ H ₁₉ O ₆		331.1188 (1.2)	9
B ₅ : 355; C ₂₀ H ₁₉ O ₆		355.1190 (1.4)	11
B ₆ : 371; C ₂₀ H ₁₉ O ₇		371.1139 (1.4)	9
B ₇ : 329; C ₁₇ H ₁₃ O ₇		329.0668 (1.1)	11
B ₈ : 357; C ₂₀ H ₂₁ O ₆		357.1346 (1.3)	10
C ₁ : 295; C ₁₄ H ₁₅ O ₇		295.0823 (1.1)	6
C ₂ : 323; C ₁₆ H ₁₉ O ₇		323.1136 (1.1)	6
C ₃ : 325; C ₁₅ H ₁₇ O ₈		325.0929 (1.1)	6
C ₄ : 353; C ₁₇ H ₂₁ O ₈		353.1241 (1.1)	6

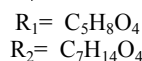
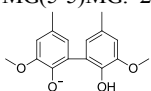
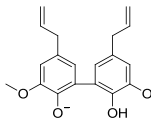
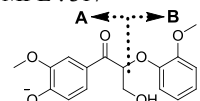
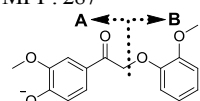


Table 3. Deprotonated molecules formed upon negative-ion mode ESI from dimeric lignin model compounds, the fragment ions of the deprotonated molecules with their relative abundances, and the fragment ions' fragment ions with their relative abundances, formed in consecutive ion isolation/CAD experiments.^a

Model Compounds (m/z of [M-H] ⁻)	MS ² /CAD Product Ions (m/z) and Their Relative Abundances	MS ³ /CAD Product Ions ^a (m/z) and Their Relative Abundances
MG(5-5)MG: 273 	273-CH ₃ (258) 100%	258-CH ₃ (243) 100% 258-H ₂ O (240) 40% 258-COH (229) 15%
E(5-5)E: 325 	325-CH ₃ (310) 100%	310-CH ₃ (295) 100% 310-OH (293) 65% 310-H-H ₂ O (291) 56% 310-C ₃ H ₅ (269) 48% 310-CH ₃ -H (294) 48% 310-CH ₃ -C ₃ H ₅ (254) 35% 310-H (309) 31% 310-COH (281) 24%
MPE : 317 	317-CH ₂ O (287) 100% 317-B-H (193) 64% 317-B (194) 10%	287-CH ₃ (272) 100% 287-B (179) 32% 287-CH ₃ -B (164) 12% 287-A (123) 10%
MPP: 287 	287-CH ₃ (272) 100% 287-B (164) 10%	272-B (149) 100% 272-A (136) 27% 272-B-CO (121) 14% 272-A-CO (163) 7%

^a MS³ was performed only for the most abundant product ion in the MS² spectra to avoid sacrificing the duty cycle of the instrument.

Table 4. Deprotonated molecules formed upon negative-ion mode ESI from unknown analytes in organosolv switchgrass mixture, and the fragment ions of the deprotonated molecules with their relative abundances, and the fragment ions' fragment ions with their relative abundances, formed in consecutive ion isolation/CAD experiments. ^a Proposed structures are shown.

Proposed Ion Structures and their m/z	MS ² /CAD Product Ions (m/z) and Their Relative Abundances	MS ³ /CAD Product Ions ^a (m/z) and Their Relative Abundances
A₁₀ : 193 	193-H (192) 100% 193-COH (164) 66% 193-CH ₃ (178) 63% 193-COH-H (163) 19%	192-CO (164) 100% 192-COH (163) 25%
B₁ : 303 	303- HCOOH (257) 100% 303-H ₂ O (285) 92% 303-CH ₃ -H ₂ O (270) 54% 303-CO (275) 35% 303-CH ₃ (288) 26%	257-CH ₃ (242) 100% 257-CH ₂ O (227) 77% 257-CH ₃ OH (225) 18% 257-CO ₂ (213) 11%
B₂ : 339 	339- CH ₂ O (309) 100% 339-CH ₃ (324) 22% 339- CH ₂ O-CH ₃ (294) 15%	309-CH ₃ (294) 100%
B₃ : 273 	273-CH ₃ (258) 100%	258-CH ₃ (243) 100% 258-H ₂ O (240) 10% 258-COH (229) 9%
B₄ : 331 	331- C ₂ H ₆ O (285) 100%	285-CO (257) 100% 285-CO+H ₂ O (275) 38%
B₅ : 355 	355-CH ₃ (340) 100%	340-H ₂ O (322) 100% 340-CH ₃ (325) 87% 340-C ₃ H ₇ O (281) 21% 340-COH (311) 21% 340-CO ₂ (296) 17%
B₇ : 329 	329-CH ₃ (314) 100%	314-CH ₃ (299) 100%
B₈ : 357 	357-CO ₂ (313) 100% 357-CH ₃ (342) 54% 357-B (209) 39% 357-CO ₂ -CH ₃ (298) 34% 357-A (147) 25%	313-CH ₃ (298) 100%
C₁ : 295 C₂ : 323 	295-C ₂ H ₄ O ₂ (235) 100% 295-C ₃ H ₆ O ₃ (205) 8%	235-C ₃ H ₄ O ₂ (163) 100%
C₃ : 325 C₄ : 353 	323-C ₇ H ₁₄ O ₅ (145) 100% 323-C ₇ H ₁₆ O ₆ (163) 12%	145-CO (117) 100%
C₃ : 325 C₄ : 353 	325-C ₂ H ₄ O ₂ (265) 100% 325-C ₃ H ₆ O ₃ (235) 19% 325-C ₃ H ₈ O ₄ (217) 7% 325-C ₃ H ₈ O ₄ (193) 9%	265-C ₃ H ₄ O ₂ (193) 100%
R ₁ = C ₅ H ₈ O ₄ R ₂ = C ₇ H ₁₄ O ₄	353-C ₇ H ₁₄ O ₅ (175) 100% 353-C ₇ H ₁₄ O ₅ -CH ₃ (160) 16% 353-CH ₃ (338) 15% 353-C ₇ H ₁₆ O ₆ (193) 12%	175-CH ₃ (160) 100%

^a MS³ was performed only for the most abundant product ion in the MS² spectra to avoid sacrificing the duty cycle of the instrument.

Acknowledgements

This work was supported as part of the Center for Direct Catalytic Conversion of Biomass to Biofuels (C3Bio), an Energy Frontier Research Center funded by the U.S. Department of Energy, Office of Science, Office of Basic Energy Sciences under Award Number DE-SC0000997.

References

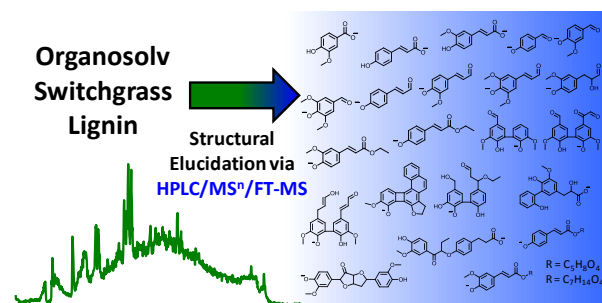
1. M. Chang, *Curr. Opin. Chem. Biol.*, 2007, 11, 677-684.
2. C. N. Hamelinck, G. van Hooijdonk and A. P. C. Faaij, *Biomass Bioenergy*, 2005, 28, 384-410.
3. H. Hisano, R. Nandakumar and Z.-Y. Wang, *In Vitro Cell. Dev. Bio-Plant*, 2009, 45, 306-313.
4. D. Mohan, C. U. Pittman, Jr. and P. H. Steele, *Energy Fuels*, 2006, 20, 848-889.
5. E. K. Pye and M. Rushton, in *Catalytic Process Development for Renewable Materials*, eds. P. Imhof and J. C. v. d. Waal, Wiley-VCH Verlag GmbH & Co., KGaA, Weinheim, Germany, 1 edn., 2013, pp. 239-263.
6. A. Ragauskas, C. Williams, B. Davison, G. Britovsek, J. Cairney, C. Eckert, W. Frederick, J. Hallett, D. Leak, C. Liotta, J. Mielenz, R. Murphy, R. Templer and T. Tschaplinski, *Science*, 2006, 311, 484-489.
7. M. J. d. I. Torre, A. Moral, M. D. Hernández, E. Cabeza and A. Tijero, *Ind. Crop. Prod.*, 2013, 45, 58-63.
8. J.-K. Weng, X. Li, N. Bonawitz and C. Chapple, *Curr. Opin. Biotechnol.*, 2008, 19, 166-172.
9. J. Zakzeski, P. C. A. Bruijninx, A. L. Jongerius and B. M. Weckhuysen, *Chem. Rev.*, 2010, 110, 3552-3599.
10. J. J. Bozell, *BioResources*, 2010, 5, 1326-1327.
11. F. Cherubini and A. H. Stromman, *Energy Fuels*, 2010, 24, 2657-2666.
12. F. Calvo-Flores and J. Dobado, *ChemSusChem*, 2010, 3, 1227-1235.
13. Z. Zhu, *Am. J. Biomed. Sci.*, 2013, 5, 59-68.
14. S. B. S. McLaughlin, R.; Bransby, D.; Wiselogle, A., 1996.
15. J. J. Bozell, S. K. Black, M. Myers, D. Cahill, W. P. Miller and S. Park, *Biomass Bioenergy*, 2011, 35, 4197-4208.
16. M. Oliet, J. García, F. Rodríguez and M. A. Gilarranz, *Chem. Eng. J.*, 2002, 87, 157-162.
17. E. Pye and J. Lora, *Tappi J.*, 1991, 74, 113-118.
18. J. Bozell, C. O'Lenick and S. Warwick, *J. Agric. Food Chem.*, 2011, 59, 9232-9242.
19. S. K. Hanson, R. T. Baker, J. C. Gordon, B. L. Scott and D. L. Thorn, *Inorg. Chem.*, 2010, 49, 5611-5618.
20. I. Hasegawa, Y. Inoue, Y. Muranaka, T. Yasukawa and K. Mae, *Energy Fuels*, 2011, 25, 791-796.
21. H. Meyermans, K. Morreel, C. Lapierre, B. Pollet, A. De Bruyn, R. Busson, P. Herdewijn, B. Devreese, J. Van Beeumen, J. Marita, J. Ralph, C. Chen, B. Burggraeve, M. Van Montagu, E. Messens and W. Boerjan, *J. Biol. Chem.*, 2000, 275, 36899-36909.
22. T. H. Parsell, B. C. Owen, I. Klein, T. M. Jarrell, C. L. Marcum, L. J. Hauptert, L. M. Amundson, H. I. Kenttämaa, F. Ribeiro, J. T. Miller and M. M. Abu-Omar, *Chem. Sci.*, 2013, 4, 806-813.
23. X. Li, J.-K. Weng and C. Chapple, *Plant J.*, 2008, 54, 569-581.
24. N.-E. E. Mansouri, F. Vilaseca and J. Salvadó, *J. Appl. Polym. Sci.*, 2012, 126, 214-221.
25. P. M. Mayer and C. Poon, *Mass Spectrom. Rev.*, 2009, 28, 608-639.
26. S. A. McLuckey, *J. Am. Soc. Mass Spectrom.*, 1992, 3, 599-614.
27. L. Sleno and D. A. Volmer, *J. Mass Spectrom.*, 2004, 39, 1091-1112.

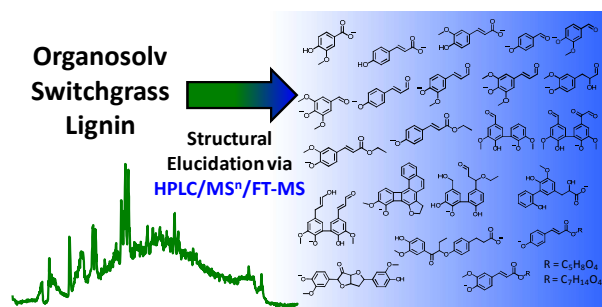
28. J.-L. Wen, B.-L. Xue, S.-L. Sun and R.-C. Sun, *J. Chem. Technol. Biotechnol.*, 2013, 88, 1663-1671.
29. D. A. Skoog, F. J. Holler and S. R. Crouch, *Principles of Instrumental analysis*, Thomson Brooks/Cole, Belmont, CA, 2007.
30. J. T. Watson and O. D. Sparkman, *Introduction to Mass Spectrometry: Instrumentation, Applications, and Strategies for Data Interpretation*, Wiley & Sons, West Sussex, England, 4 edn., 2008.
31. L. J. Hauptert, B. C. Owen, C. L. Marcum, T. M. Jarrell, C. J. Pulliam, L. M. Amundson, P. Narra, M. S. Aqueel, T. H. Parsell, M. M. Abu-Omar and H. I. Kenttämäa, *Fuel*, 2012, 95, 634-641.
32. B. C. Owen, L. J. Hauptert, T. M. Jarrell, C. L. Marcum, T. H. Parsell, M. M. Abu-Omar, J. J. Bozell, S. K. Black and H. I. Kenttämäa, *Anal. Chem.*, 2012, 84, 6000-6007.
33. R. G. Cooks, K. L. Busch and G. L. Glish, *Science*, 1983, 222, 273-291.
34. L. Amundson, B. Owen, V. Gallardo, S. Habicht, M. Fu, R. Shea, A. Mossman and H. Kenttämäa, *J. Am. Soc. Mass Spectrom.*, 2011, 22, 670-682.
35. J. W. Amy, W. E. Baitinger and R. G. Cooks, *J. Am. Soc. Mass Spectrom.*, 1990, 1, 119-128.
36. L. L. Lopez, P. R. Tiller, M. W. Senko and J. C. Schwartz, *Rapid Commun. Mass Spectrom.*, 1999, 13, 663-668.
37. F. W. McLafferty, *Int. J. Mass Spectrom.*, 2001, 212, 81-87.
38. E. Kiyota, P. Mazzafera and A. Sawaya, *Anal. Chem.*, 2012, 84, 7015-7020.
39. K. Morreel, O. Dima, H. Kim, F. Lu, C. Niculaes, R. Vanholme, R. Dauwe, G. Goeminne, D. Inzé, E. Messens, J. Ralph and W. Boerjan, *Plant Physiol.*, 2010, 153, 1464-1478.
40. K. Morreel, H. Kim, F. Lu, O. Dima, T. Akiyama, R. Vanholme, C. Niculaes, G. Goeminne, D. Inzé, E. Messens, J. Ralph and W. Boerjan, *Anal. Chem.*, 2010, 82, 8095-8105.
41. C. Vafiadi, E. Topakas, K. K. Y. Wong, I. D. Suckling and P. Christakopoulos, *Tetrahedron: Asymmetry*, 2005, 16, 373-379.
42. S. Kawai, K. Okita, K. Sugishita, A. Tanaka and H. Ohashi, *J. Wood Sci.*, 1999, 45, 440-443.
43. F. A. Marques, F. Simonelli, A. R. M. Oliveira, G. L. Gohr and P. C. Leal, *Tetrahedron Lett.*, 1998, 39, 943-946.
44. J. J. Bozell, C. J. O'Lenick and S. Warwick, *J. Agric. Food Chem.*, 2011, 59, 9232-9242.
45. M. C. Y. Chang, *Curr. Opin. Chem. Biol.*, 2007, 11, 677-684.
46. T. Q. Yuan, S. N. Sun, F. Xu and R. C. Sun, *J. Agric. Food Chem.*, 2011, 59, 10604-10614.
47. N. R. Vinueza, V. A. Gallardo, J. F. Klimek, N. C. Carpita and H. I. Kenttämäa, *Carbohydr. Polym.*, 2013, 98, 1203-1213.
48. W. J. Connors, S. Sarkanen, and J. L. McCarthy, *Holzforschung* **1980**, 3, 80-85.

Importance statement:

The major products of organosolv lignin are low molecular weight compounds, monomeric and dimeric lignin units, with various functionalities.

Contents graphic:





A method for direct structural elucidation of compounds in organosolv lignin.